JOURNAL OF MATERIALS SCIENCE 33 (1998) 2195–2202

Wear mechanism of XD^{TM} ZL201–TiB_2 *in situ* composite

B. S. LI, J. H. OUYANG, J. J. GUO, G. J. YUAN, Q. C. LI
Department of Metals and Technology, Harbin Institute of Technology, Harbin 150001, People's Republic of China

The microstructure and dry sliding wear behaviour of XD^{TM} ZL201–TiB_2 *in situ* composite were studied by scanning electron microscopy, transmission electron microscopy, X-ray diffraction, pin-on-ring friction and wear testing. The microstructural constituents of the ZL201–TiB_2 composite aged at 175 °C for various ageing times were found to be dispersive submicrometre TiB_2 particles, fine θ″, θ′-precipitates and α-Al solid solutions. As contrasted to the unreinforced ZL201 alloy, the ZL201–TiB_2 composite possessed a higher microhardness and wear-resistance as well as a shorter ageing time for peak hardness. With the increase of sliding distance, transition of the dominant wear mechanism for the ZL201–TiB_2 composite occurred from adhesive wear to fatigue wear in sliding contacts. At the earlier stages of wear, adhesive wear characteristics featured by mild scratchings and plastic smearing were observed on the worn surface and platelet-type wear debris; but at the later stages, contact fatigue failure of a relatively thick surface layer in relative motion, which revealed a build-up of layer-like structure and the presence of spherical particles of debris, became the dominant factor for the removal of composites.

1. Introduction

Because of their high strength-to-weight ratios aluminium alloys have found widespread use in transportation engineering applications. However, the relatively low wear resistance of aluminium alloys is one of the major factors that restrict their potential tribological applications in automotive components including engine blocks, piston rings and brake rotors. An important approach to producing potentially wear-resistant Al alloys is to add hard ceramic particles, such as SiC, Al_2O_3, TiC or ZrO_2, that also improve the elastic modulus and strength of the matrix alloys [1–7]. In previous investigations [8], interfacial bonding between hard ceramic reinforcements and the matrix was verified to be a control factor whether a remarkable improvement of wear resistance of the composites could be acquired or not. If the reinforcements were well bonded to the matrix, the composite wear resistance increased continuously with increasing volume fraction of ceramic particles. Otherwise, critical limit enhanced wear resistance will be attained and thereafter this start will to decrease.

Wear debris generated by different wear mechanisms has been found to be characteristic of the specific wear mechanism and have been distinguished from one another. Scott and co-workers studies on debris examination [9–12] and Yang and co-workers paper [13] on modelling the wear processes in sliding friction revealed a prognostic approach to failure prevention of steels. Similar methods can be used for effective failure investigation of Al-based composites.

In the present paper, the exthermic disperation (XD^{TM}) process was used for fabricating ZL201–TiB_2 *in situ* composites, especially because of the stable and clean interfaces and better properties obtained. The microstructure, wear debris and wear mechanism of the XD^{TM} ZL201–TiB_2 *in situ* composite were studied using a dry sliding friction and wear testing machine.

2. Experimental procedure

2.1. Preparation of materials

The composite material studied in this work was an Al–Cu–Mn–Ti alloy (ZL201) reinforced with 15 wt% TiB_2 particles. The chemical composition of the matrix alloy powder, with an average size of 38.5 μm, was in weight per cent 4.5–5.3 Cu, 0.6–1.0 Mn and 0.15–0.35 Ti, and its geometry appeared to be spherical. The ZL201–TiB_2 composite was fabricated using XD^{TM} techniques. The ZL201 alloy powder was dry-mixed with titanium and boron powders, having average sizes of 53 and 1 μm, respectively, according to the required proportion, and then was cold isostatically pressed, and finally sintered in a vaccum furnace after degassing. The reaction taking place among several original powders produced an XD^{TM} master alloy with a high volume fraction of TiB_2 particles. The XD^{TM} master alloy was diluted with melted ZL201 alloy to acquire a ZL201–15 wt % TiB_2 composite.

The ZL201–TiB_2 composite was cut into samples $4 \times 10 \times 20$ mm in size that were solution treated at 535 °C for 1 h, and finally followed by ageing at 175 °C

for 4, 9, 15 and 26 h, respectively. The matrix alloy was given the same heat treatment before wear testing. The specific gravities of the unreinforced ZL201 alloy and ZL201–TiB_2 were measured as 2.78 and 3.04 $g\,cm^{-3}$, respectively.

2.2. Microstructural observation and wear test

The microstructure of the samples was observed by an S-570 type scanning electron microscope (SEM), a Phillips SM-12 type transmission electron microscope (TEM) and D/max-rB type X-ray diffractometer (XRD) techniques. The wear test was carried out without lubrication at room temperature using a pin-on-ring friction and wear testing machine. The ring of wear couple was made of AISI 521 000 steel with a hardness of HRC60. The wear conditions were given as 70 N normal load, 1.47 $m\,s^{-1}$ sliding speed and 45–270 m sliding distance. The morphologies of the worn surface and wear debris were examined using an S-570 SEM.

3. Results and discussion

3.1. Microstructure

The mechanism of the combustion reaction for the Al–Ti–B system indicated that the addition of aluminium decreased the ignition temperature of the Ti–B reaction as a solvent. Drastic combustion reaction began with the melting of aluminium alloy powder, and then a sequence of Al–Ti intermetallic compounds were produced, which was followed by reaction between Ti and B. With dissolution of intermetallic compounds during heating, TiB_2 particles nucleated independently *in situ* and grew. To acquire a ZL201–TiB_2 composite without Al–Ti intermetallic compounds, optimum processing conditions were used in the present study. Fig. 1 shows the XRD patterns of the ZL201 alloy and ZL201–TiB_2 composite as-cast.

After ageing at 175 °C for various times, fine θ″ and θ′ precipitates were observed in the samples of both the ZL201 alloy and the ZL201–TiB_2 composite. The microstructural characteristics of the ZL201–TiB_2 composite aged at 175 °C for 9 h are given in Fig. 2. It can be seen that fine TiB_2 particles with an average size of 0.2 μm are distributed dispersively in the ZL201–TiB_2 composite. The bonding interface between the TiB_2 particles and α-Al was stable and clean without any pollution. The precipitates in the ZL201–TiB_2 composite aged at 175 °C for 9 h consist of a large number of θ″ precipitates and small quantities of θ′ precipitates. Because of the formation of a large number of coherent θ″ precipitates, the highly strained matrix around the θ″ precipitates can be observed distinctly in Fig. 2c. From Fig. 2d, fine well defined θ′ precipitates are generally regularly oriented in the α-Al matrix. The precipitation of incoherent θ′ phases relieved the strain energy around precipitates and no distinctly strained matrix can be observed in Fig. 2d. As the ageing time continued to increase, the magnitude of the θ″ phases gradually decreased, while the θ′ phases continued to precipitate and grow in α-Al solid solution. In the ZL201–TiB_2 composite aged at 175 °C for 26 h, the magnitude and size of the θ′ phases become large; however, no stable θ-Al_2 Cu precipitate can be found.

3.2. Wear behaviour of the ZL201–TiB_2 composite

The wear volume and wear rate of ZL201 alloy and ZL201–TiB_2 composites aged at 175 °C for various ageing times are shown in Fig. 3. From Fig. 3 it is demonstrated that the wear resistance of composites improves remarkably with the incorporation of reinforcements. *In situ* formation of a TiB_2 particle in the composite decreased significantly the wear volume and wear rate of ZL201–TiB_2 pin samples. Fig. 3 also deals with the effect of ageing time on the wear resistance of two kinds of materials. Under the same wear condition, the ZL201–TiB_2 composite aged at 175 °C for 9 h exhibited the highest wear resistance to the AISI 521 000 steel ring, while the ZL201 alloy aged at 175 °C for 15 h has a better wear resistance than that aged at 175 °C for other ageing times. Fig. 4 shows how the hardness of the pin samples varies as function of ageing time. As the ZL201 alloy and the ZL201–TiB_2 composite are aged at 175 °C, GP zones are unstable and the first precipitate to form is θ″. The volume fraction of θ″ increases with time causing the

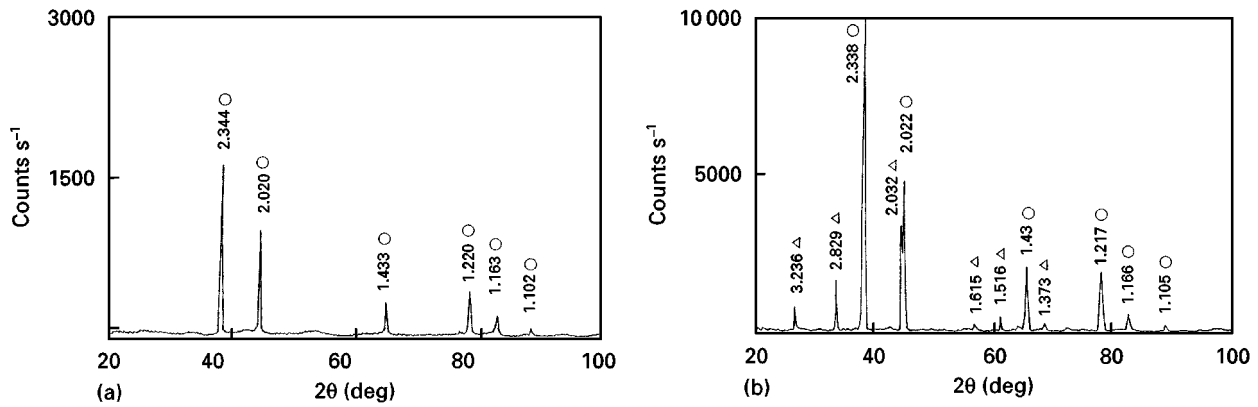

Figure 1 XRD patterns of ZL201 alloy and ZL201–TiB_2 composite as cast: (a) ZL201 alloy and (b) ZL201–TiB_2 composite. (○) Al, (△) TiB_2.

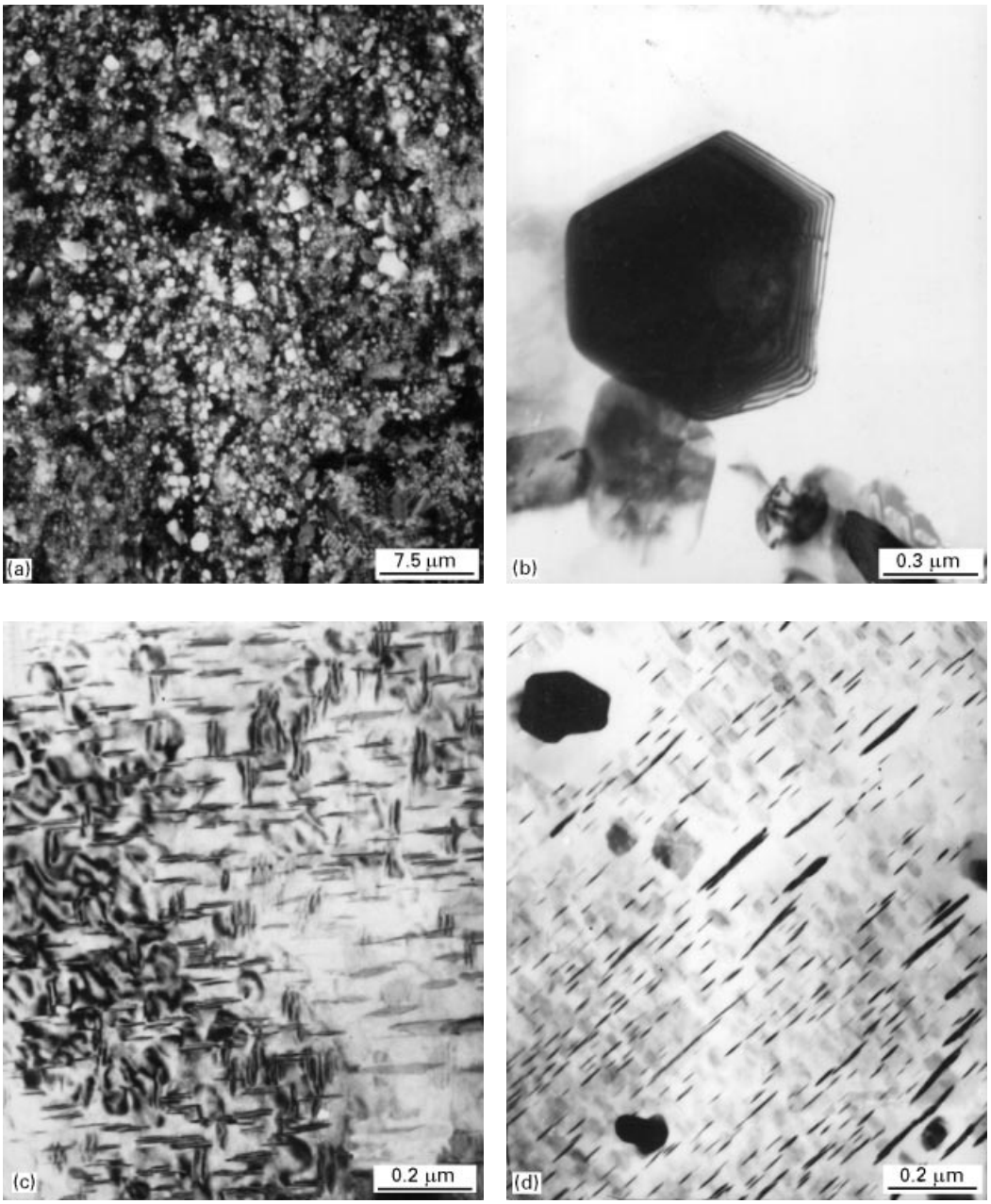

Figure 2 Microstructural characteristics of the ZL201–TiB_2 composite aged at 175 °C for 9 h: (a) distribution of TiB_2 particles (SEM), (b) TiB_2 particle in α-Al (TEM), (c) θ″ precipitate in α-Al (TEM), and (d) θ′ precipitate in α-Al (TEM).

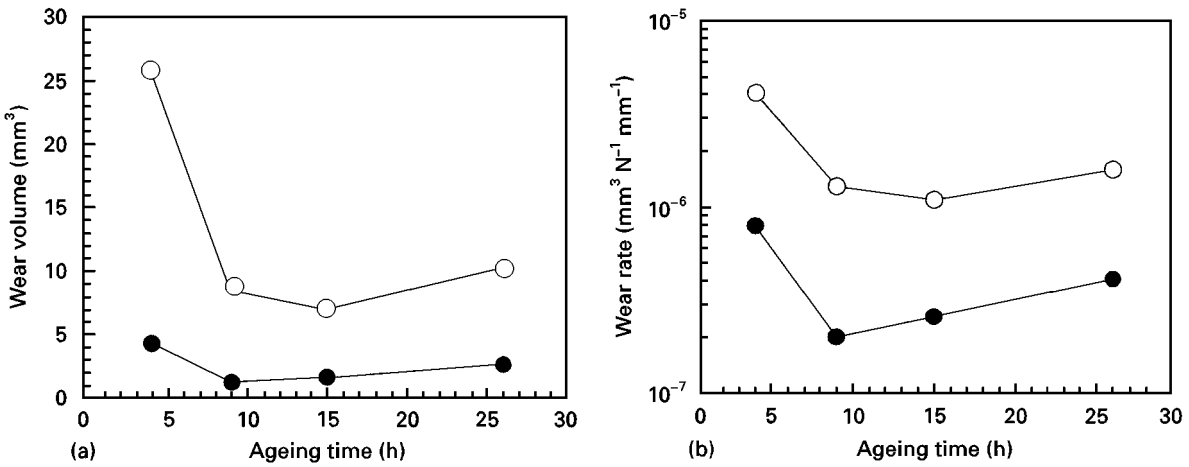

Figure 3 Wear volume (a) and wear rate (b) of ZL201 alloy (○) and ZL201–TiB_2 composite (●) aged at 175 °C for various ageing times ($P = 70$ N, $V = 1.47\ m\ s^{-1}$ and $L = 90$ m).

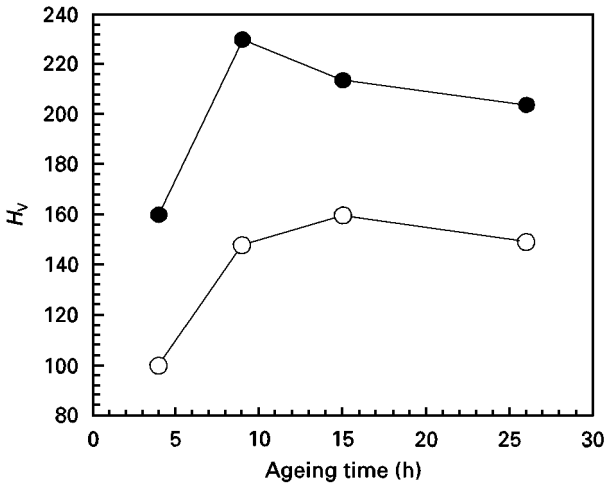

Figure 4 Hardness of ZL201 alloy (○) and ZL201–TiB_2 composite (●) versus ageing time.

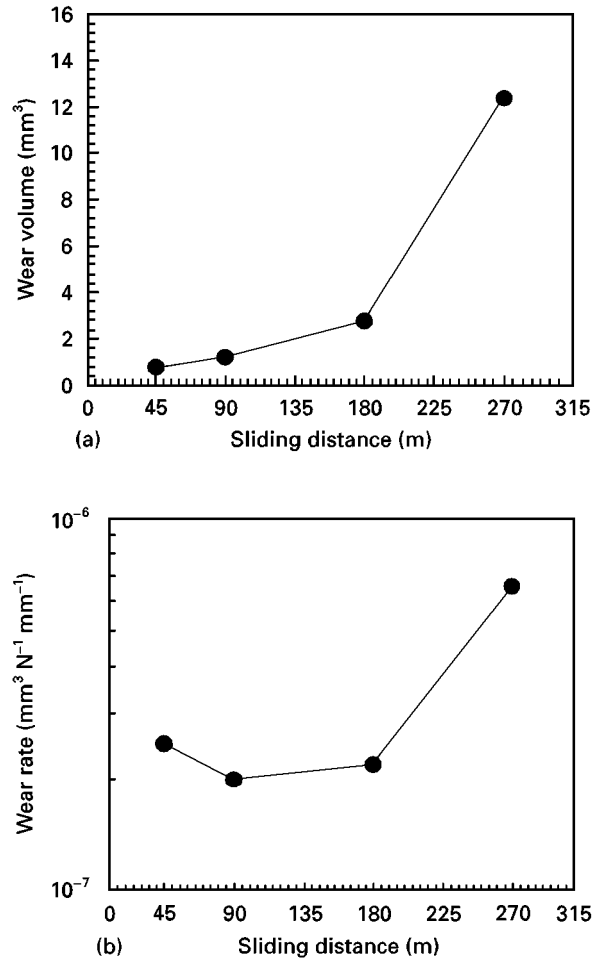

Figure 5 Wear volume (a) and wear rate (b) of ZL201–TiB_2 composite aged at 175 °C for 9 h versus sliding distance ($P = 70$ N and $V = 1.47$ m s^{-1}).

hardness to increase because the dislocations must be forced through the highly strained matrix that results from the misfit perpendicular to the θ″ plates. Eventually, with the formation of θ′, the spacing between the precipitates becomes so large that the dislocations are able to bow and the hardness begins to decrease. Maximum hardness is associated with a combination of θ″ and θ′. The incorporation of TiB_2 particles enhances the peak hardness of the composite and shortens the ageing time for peak hardness from 15 h for ZL201 alloy to 9 h for the ZL201–TiB_2 composite.

From Figs 3 and 4 it can be found that the peak-hardness of pin samples for the two kinds of material is consistent with the samples' minimum wear volumes and wear rates.

Fig. 5 shows how the wear volume and wear rate of the ZL201–TiB_2 composite aged at 175 °C for 9 h varies with the increase of sliding distance. A slow increase of wear volume is found at earlier stages of the wear process, but as the sliding distance increases beyond 180 m, the wear volume of the pin sample exhibits a rapid increase. The same results can be obtained from the plot of wear rate shown in Fig. 5b; when the sliding distance increase was from 180 to 270 m, the wear rate increases from 2.2×10^{-7} to 6.6×10^{-7} mm^3 N^{-1} mm^{-1}. This great increase in wear rate is associated with the transition of a dominant wear mechanism during wear.

3.3. Worn surface and wear debris analysis

The morphology of the worn surfaces of the two kinds of materials aged at 175 °C for 15 h is shown in Fig. 6, only mild wear with fine scratching is observed on the worn surface of the TiB_2-reinforced composite. However, severe plastic deformation and adhesive wear, with a scale-like feature caused by extensive shear, are found on the worn surface of the ZL201 alloy. From Fig. 6a, fine TiB_2 particles are distributed dispersively on the worn surface. This demonstrates that fine TiB_2 particles enhance the resistance to plastic smearing and removal of the edges of grooves during subsequent passes. As a result the ZL201–TiB_2 composite possesses a much higher resistance to plastic deformation and scoring.

The morphology of the wear debris of the two kinds of materials aged at 175 °C for 15 h are shown in Fig. 7. The wear debris from the ZL201 alloy shows platelet type adhesive wear particles that are much larger than those from the ZL201–TiB_2 composite. A typical scale-like feature and scuffings caused by extensive shear can be observed distinctly on the surface of the wear debris. From the morphology and size of the wear debris, the TiB_2 particles can serve as hard barriers that enhance the resistance to plastic deformation and relieve delamination and transfer of the massive matrix.

Fig. 8 shows how the morphology of the worn surface of the ZL201–TiB_2 composite aged at 175 °C for 9 h varies with increasing sliding distance under the wear condition of 70 N normal load and 1.47 m s^{-1} sliding speed. At the earlier stages of the wear process ($L = 45$ m), only fine scratchings can be observed on the worn surface. As the sliding distance increases to 90 m, no distinct coarsening of scratchings and plastic deformation of matrix are seen on the worn surface. But when the sliding distance increases to 180 m, spherical wear particles and tongues of metals are observed on the surface as well as distinct plastic deformation and transfer of the matrix caused by wear couple. The spherical particles of debris have

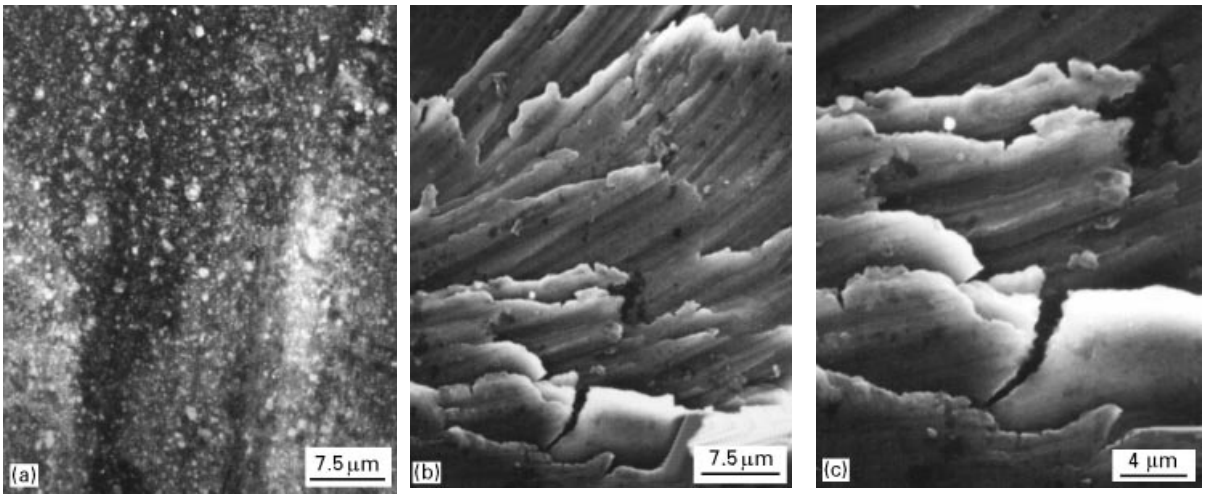

Figure 6 Morphology of the worn surfaces of the two kinds of materials aged at 175 °C for 15 h ($P = 70$ N, $V = 1.47$ m s^{-1} and $L = 90$ m): (a) ZL201–TiB_2 composite; (b) ZL201 alloy; and (c) high magnification image of (b).

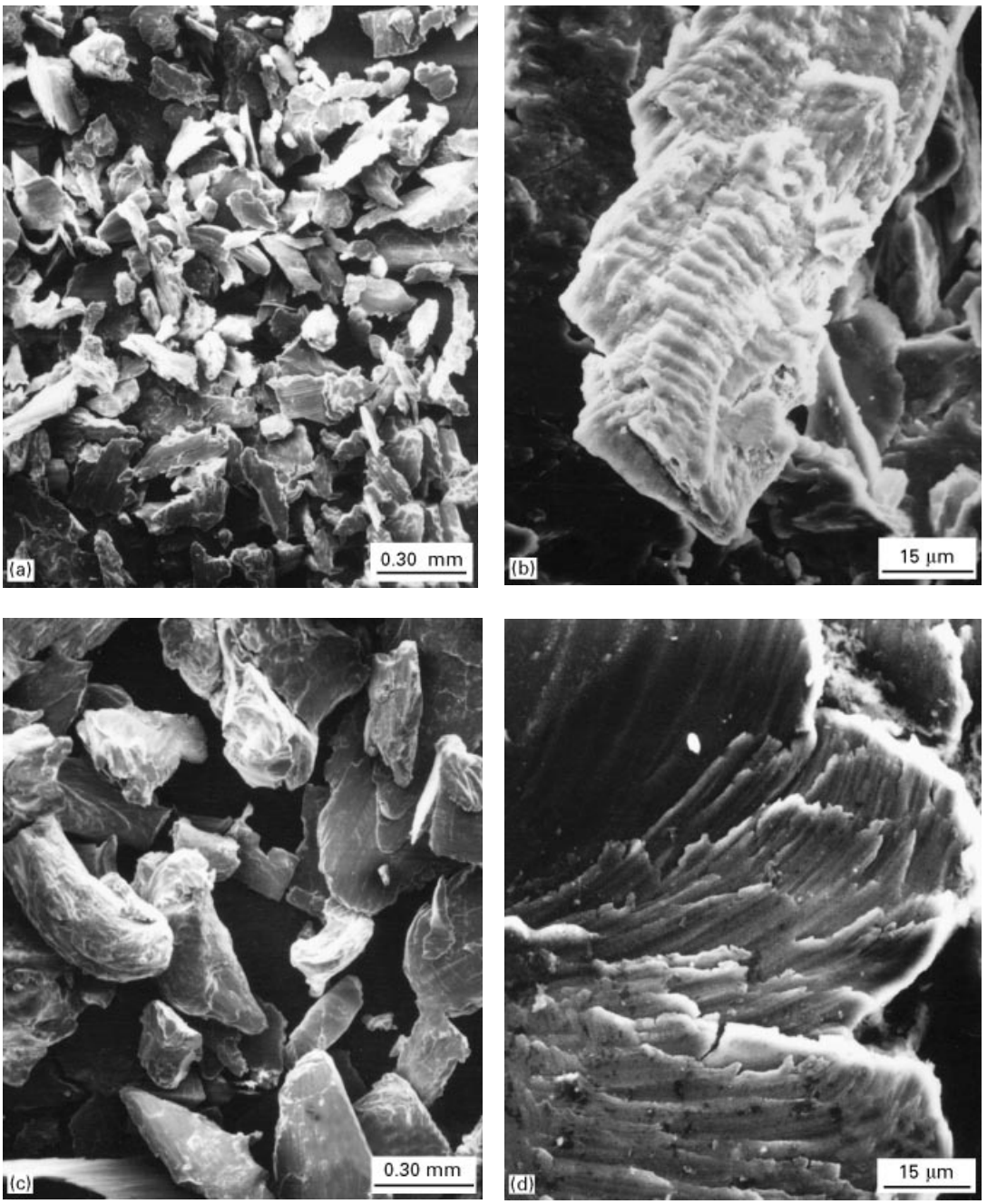

Figure 7 Morphology of wear debris of the two kinds of materials aged at 175 °C for 15 h ($P = 70$ N, $V = 1.47$ m s^{-1} and $L = 90$ m): (a, b) ZL201–TiB_2, and (c, d) ZL201 alloy.

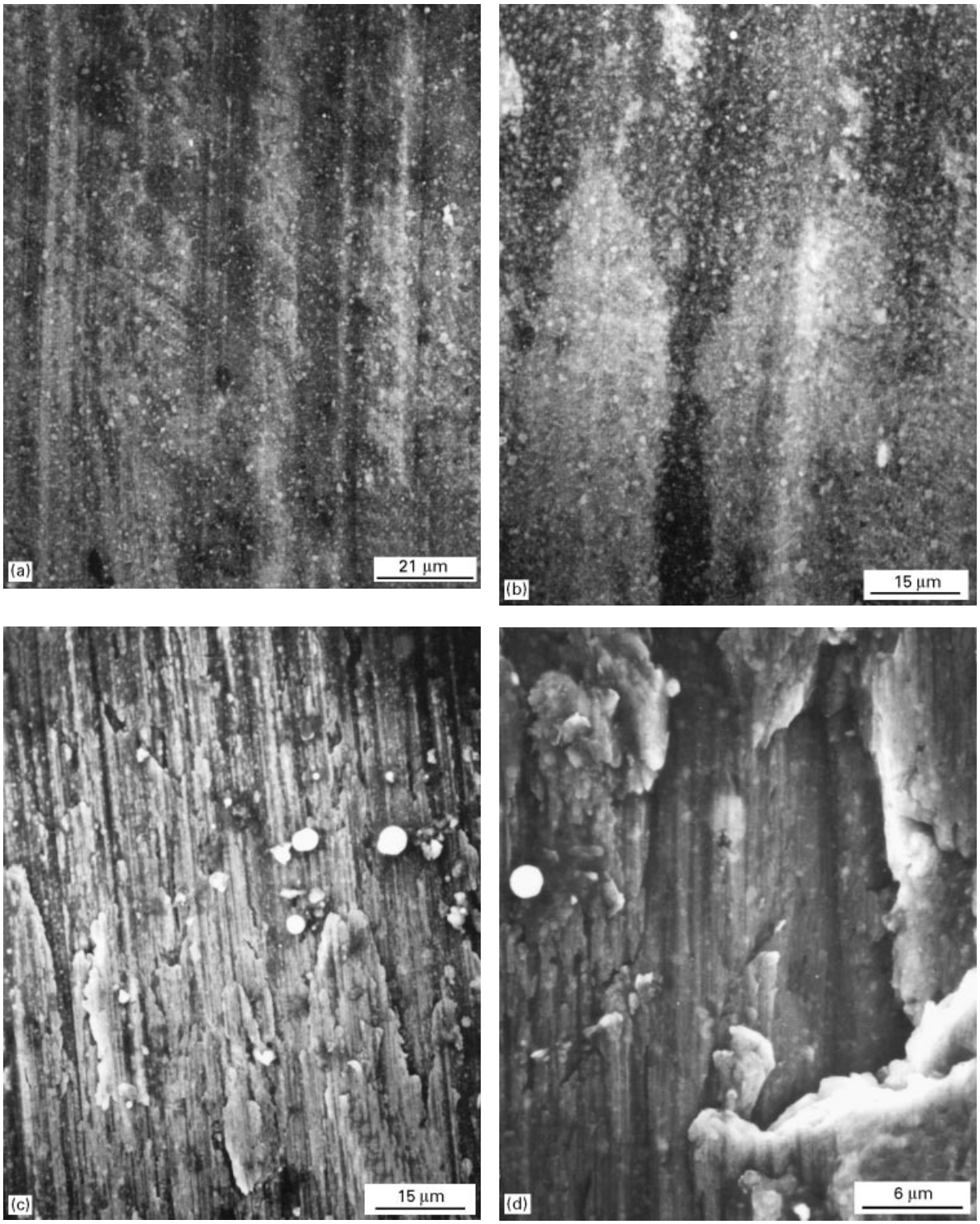

Figure 8 Morphology of the worn surface of the ZL201–TiB_2 composite aged at 175 °C for 15 h under the wear conditions of various sliding distance ($P = 70$ N and $V = 1.47$ m s^{-1}): (a) $L = 45$ m, (b) $L = 90$ m, (c) $L = 180$ m and (d) $L = 270$ m.

a layer-like structure, which is indicative of the probable mechanism of formation i.e. rolling or balling-up of tongues of metal. Such findings have been confirmed in several instances, and some spheres have a smooth surface appearance. Both the smooth surface appearance and the layered nature of some spheres are characteristic features associated with rolling and sliding contact fatigue [8–12]. A lot of spherical wear debris produced by contact fatigue wear mechanism are detected to be mainly composed of aluminium and small quantities of elements, such as copper and titanium, use X-ray energy analysis in the SEM. When the sliding distance increases to 270 m, pieces of metal can be severely worked and rounded by pressure on the fracture faces. Spherical particles may also be formed directly in deformed subsurface material by subsurface shear crack propagation. From Fig. 8d, the edges of scratchings and scuffings gradually become smooth and distinct tongues of metal partially formed into spheres are observed on the worn surface.

Morphology and EDXA results of spherical wear debris on the worn surface of the ZL201–TiB_2 com-

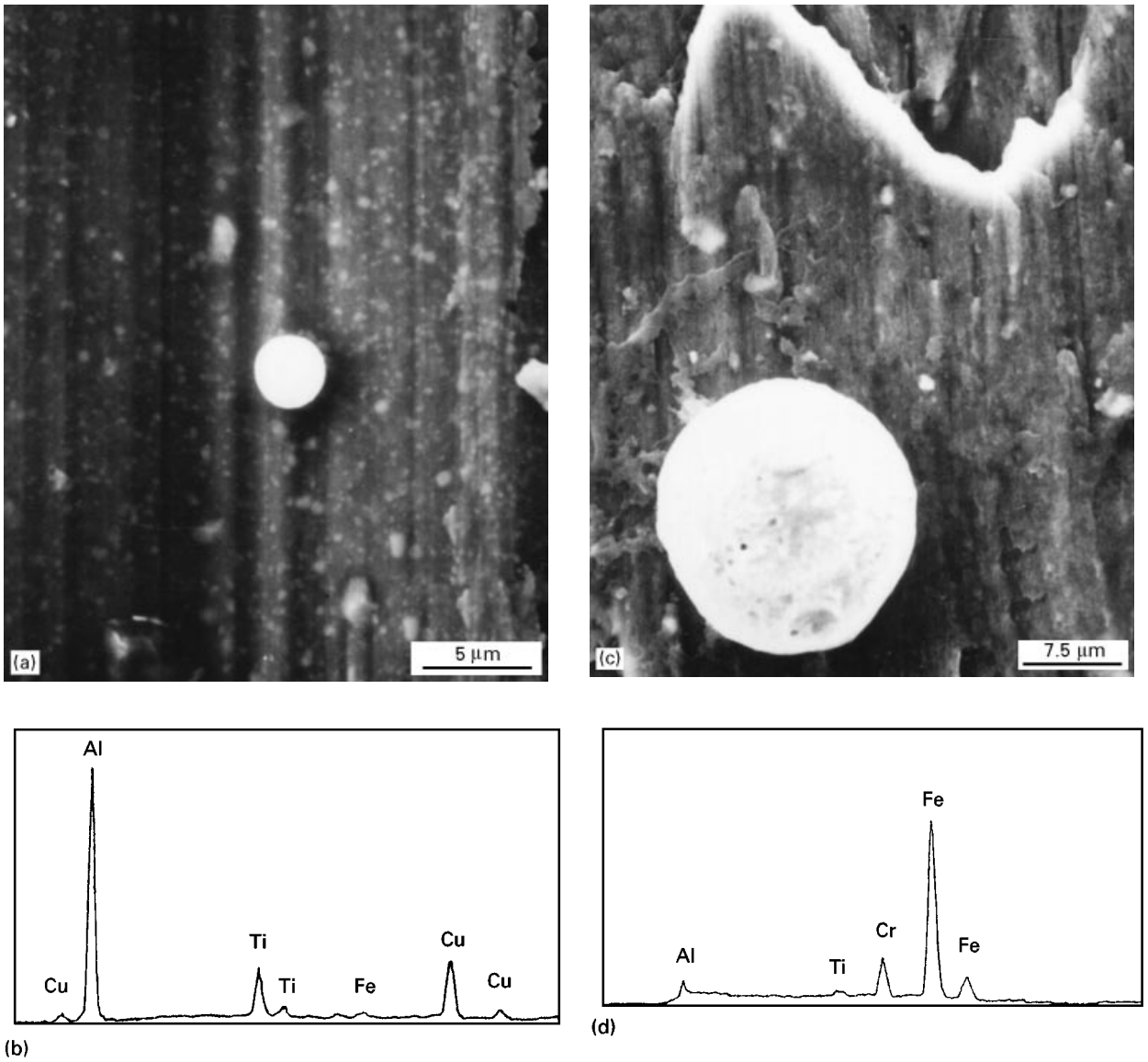

Figure 9 Morphology (a, c) and EDAX results (b, d) of spherical wear debris on the worn surface of the ZL201–TiB_2 composite: (a, b) Al spherical debris, and (c, d) Fe spherical debris.

posite are given in Fig. 9. An Fe wear sphere coming from the wear couple of AISI 521 000 steel was also examined on the worn surface, as well as an Al wear sphere coming from the pin sample. From the EDXA result, the Fe wear sphere also contains small quantities of aluminium as well as chromium. Wear seems to be dominanted by a severe contact fatigue mechanism in the relatively thick surface layer and proceeds by removal of metal in smoothing the faces of the fatigue crack.

The morphology of the wear debris caused by the contact fatigue wear mechanism in the ZL201–TiB_2 composite is given in Fig. 10. Spherical particles and smooth tongues of metal are a significant feature of the debris. The size of wear debris produced by the fatigue wear mechanism at the later stages of the wear process become larger than before. Consequently, pin samples start to be worn out abruptly. This phenomenon is consistent with the wear volume and wear rate of the ZL201–TiB_2 composite shown in Fig. 5.

4. Conclusions

1. The ZL201–TiB_2 composite aged at 175 °C for various times consists of dispersive TiB_2 particles, fine θ″, θ′ precipitates and an α-Al solid solution. The much higher wear resistance of the composite compared with the ZL201 alloy is mainly attributed to dispersive submicrometre TiB_2 particles and the high hardness of the composite.

2. The incorporation of TiB_2 particles enhances the peak hardness of the composite ageing at 175 °C and shortens the ageing time for peak hardness. The effect of the ageing time on wear resistance of the ZL201 alloy and ZL201–TiB_2 composite is very similar to that on hardness.

3. With the increase of sliding distance, transition of the dominant wear mechanism for the ZL201–TiB_2 composite occurs from adhesive wear to contact fatigue wear. At the earlier stages of wear, adhesive wear characteristics are indicated by mild scratchings and plastic smearing. At later stages, contact fatigue failure

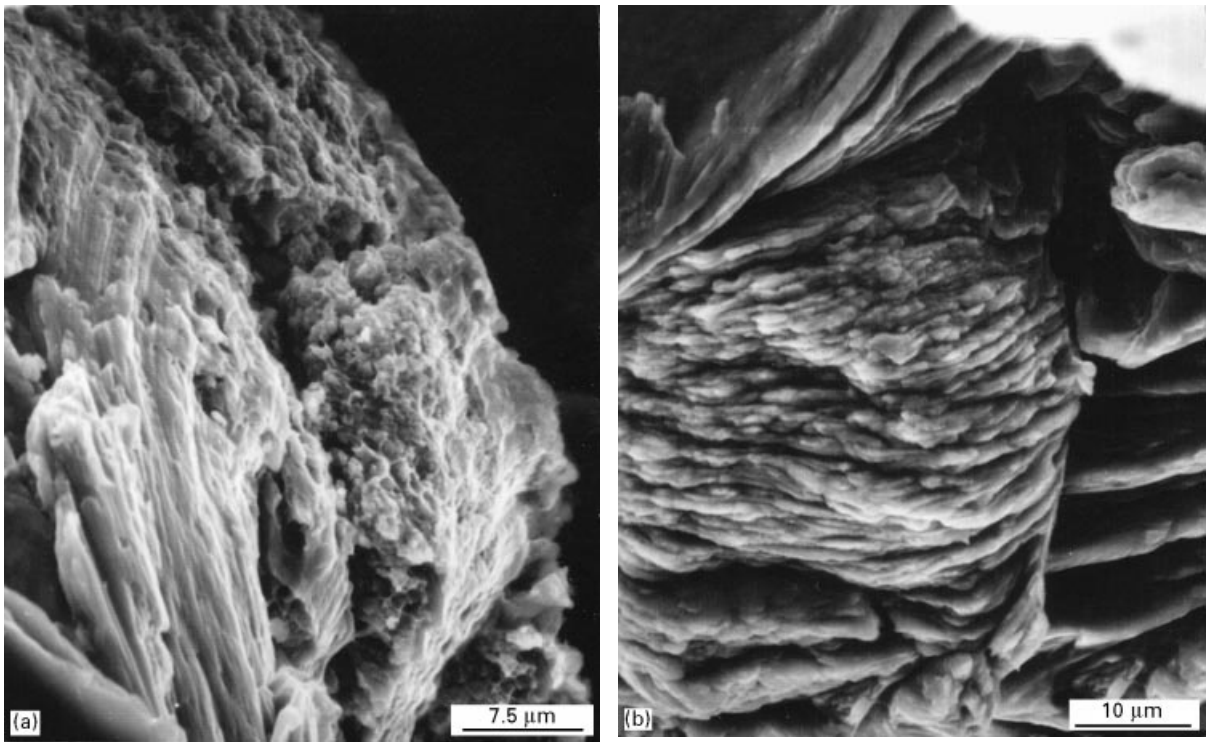

Figure 10 Morphology of wear debris caused by contact fatigue wear mechanism in the ZL201–TiB_2 composite ($P = 70$ N, $V = 1.47$ m s^{-1} and $L = 270$ m) showing (a) spherical particles, and (b) smooth tongues of metal.

of a relatively thick surface layer in relative motion, which reveals a build-up of layer-like structure and the presence of spherical particles of debris, becomes the dominant factor for removal of the composite.

References

1. R. MITRA, W. A. CHIOU, J. R. WEERTMAN and M. E. FINE, *Scripta Metall.* **25** (1991) 2689.
2. C. S. LEE, Y. H. KIM, K. S. HAN and T. LIM, *J. Mater. Sci.* **27** (1992) 793.
3. S. V. PRASAD, P. K. ROHATGI and T. H. KOSEL, *Mater. Sci. Eng.* **80** (1986) 213.
4. A. T. ALPAS and J. ZHANG, *Wear* **155** (1992) 83.
5. F. RANA and D. M. STEFANESCU, *Metall. Trans. A* **20A** (1989) 1564.
6. S. DAS, S. V. PRASAD and T. R. RAMACHANDRAN, *Wear* **133** (1989) 173.
7. C. M. FRIEND, *Scripta Metall.* **23** (1989) 33.
8. M. ROY, B. VENKATAVAMAN, V. V. BHANUPRASAD, Y. R. MAHAJAN and G. SUNDARARAJAN, *Metall. Trans. A* **23A** (1992) 2833.
9. D. SCOTT, *Wear* **34** (1975) 15.
10. D. SCOTT and G. H. MILLS, *Nature* **241** (1973) 115.
11. D. SCOTT and V. C. WESTCOTT, *Wear* **44** (1977) 173.
12. D. SCOTT and G. H. MILLS, *ibid.* **24** (1973) 235.
13. YANYI YANG, A. A. TORRANCE and P. L. B. OXLEY, *J. Phys. D, Appl. Phys.* **29** (1996) 600.

Received 25 July 1996
and accepted 5 December 1997